

Semipredictable dynamical systems

Vladimir García-Morales

Institute for Advanced Study - Technische Universität München,
Lichtenbergstr. 2a, D-85748 Garching, Germany
Departament de Termodinàmica, Universitat de València,
E-46100 Burjassot, Spain
garmovla@uv.es

A new class of dynamical systems, termed semipredictable dynamical systems, is presented. The spatiotemporal evolution of these systems have both predictable and unpredictable traits, as found in natural complex systems. We show that the dynamics of any deterministic nonlinear cellular automaton with p possible dynamical states can be decomposed at each instant of time in a unique way in a superposition of N cellular automata with p_0, p_1, \dots, p_{N-1} dynamical states each, and where the $p_{k \in \mathbb{N}}, k \in [0, N-1]$ are the N prime factors of p . These N cellular automata work on different layers of the dynamics of the original cellular automaton and even when the full spatiotemporal evolution can be unpredictable, we show that certain traits can be exactly predicted. We present an explicit example of such a system, consisting on a cellular automaton acting on a neighborhood of two sites and 12 symbols and whose rule table corresponds to the smallest Moufang loop $M_{12}(S_3, 2)$.

I. INTRODUCTION

Complex natural systems exhibit a coexistence of predictable and unpredictable traits in their dynamical evolution. This feature seems to have been excluded from mathematical investigation, perhaps because of the difficulty to state the problem rigorously or because of its suspected general mathematical intractability [1]. In this article we present a pathway to investigate the problem and in doing so discover an infinite family of systems termed *semipredictable dynamical systems* whose dynamical trajectory can be sharply separated in the ordinary sum of an exactly predictable part and a strongly unpredictable one, such that both parts can be neatly extracted from the trajectory at any time. In those systems we discover a linear superposition of a predictable layer and an unpredictable one and show how a decomposition of the dynamics can be carried out for any dynamical system modeled by a cellular automaton (CA) in order to extract these layers and make predictions. If the system is totally unpredictable, our method leads, in any case, to a reduction of the dynamics to independent layers that can be treated separately. These layers can then be linearly superimposed to get the full solution. The exciting fact is that *although the whole solution is strongly unpredictable, there are nontrivial evolving properties of it that can be exactly predicted at any time giving an explicit solution for them*.

CAAs constitute an important tool in the study of complex systems [1–6]. They have been satisfactorily used to model physical [7], chemical [8] and biological processes and, in certain cases, constitute an alternative to continuous models described by partial differential equations [9]. Natural patterns as those found in some seashells, like the Conus marmorea [10] can readily be obtained with CA [1]. Although such patterns may involve many microscopic degrees of freedom, a coarse graining of them can also be generally described by cellular automata [11, 12] and the latter can thus be used to capture the collective behavior of spatiotemporal pattern forming systems. These coarse grained models have been shown to lead to predictable patterns [11, 12]. Since coarse graining always implies that dynamical details are lost, we do not perform here any coarse graining and deal with the spatiotemporal evolution exactly. We show that, while keeping with all spatiotemporal information, it is still generally possible to make exact predictions of most complex systems whose overall spatiotemporal evolution is strongly unpredictable.

Despite involving only a finite number p of dynamical states and the interactions having a finite range ρ , already the most elementary CA can generate the highest possible complexity [1, 13]. The mathematical description of such systems in terms of discrete maps seems to have been only recently attempted [5, 14, 15] and previous researchers have mostly relied upon the computer to get insight in CA behavior. In [15] we have introduced a universal map for cellular automata which does not depend on any adjustable parameter and which is not only able to simulate Wolfram's 256 elementary CA, but any deterministic CA with any number of dynamical states. This map can also be easily extended to any number of dimensions. In [16] and [13] we have discussed some symmetries of the universal CA map that help to classify the rules into symmetry classes [16] and to understand the kind of symmetry breaking that leads to complexity at this elementary level [13].

In this article we further explore these results by making use of a digit function [17] that allows us to express the universal map for CA dynamics in a closed compact form. One major advantage of this alternative formulation is then made clear, since it allows the CA dynamics to be decomposed into simpler layers that can be separately analyzed, the spatiotemporal evolution of the CA being a linear

superposition of these layers. The outline of this article is as follows. In Section II we introduce the digit function and derive some results in which our approach is based. Then in Section III we apply these results to CAs reducing their dynamics on p symbols to a linear superposition of (generally nonlinear) CA, each acting on a reduced number $p_{k \in \mathbb{N}}$ of symbols, where the p_k 's are the prime factors of the unique prime factorization of p . Then, we present an example of a *semipredictable dynamical system* that is neither totally predictable nor totally unpredictable and analyze it through the methods introduced in this paper. Numerical computations confirm our analytical results.

II. THE DIGIT FUNCTION

The digit function, for $p \in \mathbb{N}$, $k \in \mathbb{Z}$ and $x \in \mathbb{R}$ is defined as [17]

$$\mathbf{d}_p(k, x) = \left\lfloor \frac{x}{p^k} \right\rfloor - p \left\lfloor \frac{x}{p^{k+1}} \right\rfloor \quad (1)$$

and gives the k -th digit of the real number x (when it is non-negative) in a positional numeral system in radix $p > 1$. If $p = 1$ the digit function satisfies $\mathbf{d}_1(k, x) = \mathbf{d}_1(0, x) = 0$ and it does not relate to a positional numeral system.

With the digit function we can express any real number as

$$x = \text{sign}(x) \sum_{k=-\infty}^{\lfloor \log_p |x| \rfloor} p^k \mathbf{d}_p(k, |x|) \quad (2)$$

The digit function is a staircase of p levels taking discrete integer values between 0 and $p - 1$. Each time that x is divisible by p^{k+1} the ascent of the staircase is broken and the level is set again to zero and a new staircase begins. For n and m nonnegative integers the digit function satisfies

$$\mathbf{d}_p(k, x + np^{k+1}) = \mathbf{d}_p(k, x) \quad (3)$$

$$\mathbf{d}_p(k, p^k x) = \mathbf{d}_p(0, x) \quad (4)$$

$$\mathbf{d}_p(0, \mathbf{d}_p(k, x)) = \mathbf{d}_p(k, x) \quad (5)$$

$$\mathbf{d}_p(0, n + \mathbf{d}_p(0, m)) = \mathbf{d}_p(0, n + m) \quad (6)$$

$$\mathbf{d}_p(0, n\mathbf{d}_p(0, m)) = \mathbf{d}_p(0, nm) \quad (7)$$

$$\mathbf{d}_{np}(k, x) = \mathbf{d}_p\left(k, \frac{x}{n^k}\right) + p\mathbf{d}_n\left(k, \frac{x}{p^{k+1}}\right) = \mathbf{d}_n\left(k, \frac{x}{p^k}\right) + n\mathbf{d}_p\left(k, \frac{x}{n^{k+1}}\right) \quad (8)$$

These relationships are all easy to prove. Eq. (3) and (4) follow directly from the definition. Eq. (5) follows by noting that $\mathbf{d}_p(k, x)$ is an integer $0 \leq \mathbf{d}_p(k, x) \leq p - 1$. Then

$$\mathbf{d}_p(0, \mathbf{d}_p(k, x)) = \mathbf{d}_p(k, x) - p \left\lfloor \frac{\mathbf{d}_p(k, x)}{p} \right\rfloor = \mathbf{d}_p(k, x) \quad (9)$$

since $\lfloor \mathbf{d}_p(k, x)/p \rfloor = 0$. Eq. (6) is proved by using Euclidean division, since we can always write $m = ap + b$ with a, b integers and $b = \mathbf{d}_p(0, m)$. Therefore

$$\mathbf{d}_p(0, n + \mathbf{d}_p(0, m)) = \mathbf{d}_p(0, n + ap + \mathbf{d}_p(0, m)) = \mathbf{d}_p(0, n + m) \quad (10)$$

where Eq. (3) has also been used. Eq. (7) is also proved in a similar way, using the distributive property of ordinary addition and multiplication as well. By using the definition, we have

$$\begin{aligned}\mathbf{d}_p\left(k, \frac{x}{n^k}\right) + p\mathbf{d}_n\left(k, \frac{x}{p^{k+1}}\right) &= \left\lfloor \frac{x}{p^k n^k} \right\rfloor - p \left\lfloor \frac{x}{p^{k+1} n^k} \right\rfloor + p \left\lfloor \frac{x}{p^{k+1} n^k} \right\rfloor - np \left\lfloor \frac{x}{p^{k+1} n^{k+1}} \right\rfloor \\ &= \left\lfloor \frac{x}{(np)^k} \right\rfloor - np \left\lfloor \frac{x}{(np)^{k+1}} \right\rfloor = \mathbf{d}_{np}(k, x)\end{aligned}\quad (11)$$

which proves Eq. (8).

The following result is the cornerstone of our method to decompose CA dynamics as explained in the next section. Let $p_0, p_1, \dots, p_{N-1} \in \mathbb{N}$. We have

$$\mathbf{d}_{p_0 p_1 \dots p_{N-1}}(k, x) = \sum_{h=0}^{N-1} \mathbf{d}_{p_h}\left(k, \frac{x}{(\prod_{m=0}^{h-1} p_m)^{k+1} (\prod_{n=h+1}^{N-1} p_n)^k}\right) \prod_{j=0}^{h-1} p_j \quad (12)$$

This result can easily be proved by induction. For $N = 1$, Eq. (12) is trivially valid and for $N = 2$ it reduces to Eq. (8). Let us assume the result valid for N factors. Then, for $N + 1$ factors we have, by using Eq. (8)

$$\begin{aligned}\mathbf{d}_{p_0 p_1 \dots p_N}(k, x) &= \mathbf{d}_{p_0 p_1 \dots p_{N-1}}\left(k, \frac{x}{p_N^k}\right) + p_0 p_1 \dots p_{N-1} \mathbf{d}_{p_N}\left(k, \frac{x}{(p_0 p_1 \dots p_{N-1})^{k+1}}\right) \\ &= \sum_{h=0}^{N-1} \mathbf{d}_{p_h}\left(k, \frac{x/p_N^k}{(\prod_{m=0}^{h-1} p_m)^{k+1} (\prod_{n=h+1}^{N-1} p_n)^k}\right) \prod_{k=0}^{h-1} p_k + \mathbf{d}_{p_N}\left(k, \frac{x}{(\prod_{m=0}^{N-1} p_m)^{k+1}}\right) \prod_{j=0}^{N-1} p_j \\ &= \sum_{h=0}^N \mathbf{d}_{p_h}\left(k, \frac{x}{(\prod_{m=0}^{h-1} p_m)^{k+1} (\prod_{n=h+1}^N p_n)^k}\right) \prod_{j=0}^{h-1} p_j\end{aligned}$$

which proves the validity of Eq. (12).

III. THE UNIVERSAL CA MAP, THE DECOMPOSITION OF CA DYNAMICS AND SEMIPREDICTABLE DYNAMICAL SYSTEMS

We now establish the way in which the digit function can be used to describe CA. Let us consider a 1D ring containing a total number of N_s sites. An input is given as initial condition in the form of a vector $\mathbf{x}_0 = (x_0^1, \dots, x_0^{N_s})$. Each of the x_0^j is an integer in $[0, p - 1]$ where superindex $j \in [1, N_s]$ specifies the position of the site on the 1D ring. At each t the vector $\mathbf{x}_t = (x_t^1, \dots, x_t^{N_s})$ specifies the state of the CA. Periodic boundary conditions are considered so that $x_t^{N_s+1} = x_t^1$ and $x_t^0 = x_t^{N_s}$. Let x_{t+1}^j be taken to denote the value of site j at time step $t + 1$. Formally, its dependence on the values at the previous time step is given through the mapping $x_{t+1}^j = {}^l R_p^r(x_t^{j+l}, \dots, x_t^j, \dots, x_t^{j-r})$, which we abbreviate as $x_{t+1}^j = {}^l R_p^r(x_t^j)$ [15] with the understanding that the function on the r.h.s depends on all site values within the neighborhood, with range $\rho = l + r + 1$, which contains the site j updated at the next time (l and r denote the number of cells to the left and to the right of site j respectively). We take the convention that j increases to the left. The integer number n in base 10, which runs between 0 and $p^{r+l+1} - 1$, indexes all possible neighborhood values coming from the different configurations of

site values. Each of these configurations compares to the dynamical configuration reached by site j and its r and l first-neighbors at time t and given by

$$n_t^j = \sum_{k=-r}^l p^{k+r} x_t^{j+k} \quad (13)$$

We will refer to this latter quantity often as the *neighborhood value*. The possible outputs a_n for each configuration n are also integers $\in [0, p-1]$. An integer number R can then be given in the decimal base to fully specify the rule ${}^l R_p^r$ as

$$R \equiv \sum_{n=0}^{p^{r+l+1}-1} a_n p^n. \quad (14)$$

This is the so-called Wolfram code of the CA dynamics. We now note the following, by its very definition $a_n = \mathbf{d}_p(n, R)$ denotes the output of the CA when $n_t = n$. Thus, the universal map for CA is simply given by

$$x_{t+1}^j = \mathbf{d}_p \left(\sum_{k=-r}^l p^{k+r} x_t^{j+k}, R \right) = \left\lfloor \frac{R}{p^{\sum_{k=-r}^l p^{k+r} x_t^{j+k}}} \right\rfloor - p \left\lfloor \frac{R}{p^{1+\sum_{k=-r}^l p^{k+r} x_t^{j+k}}} \right\rfloor \quad (15)$$

All deterministic 1D first-order-in-time CA are given by Eq. (15) for any neighborhood range and number of symbols. With this advantageous compact form for the universal map we do not need to give any table of configurations as input for the CA but just only the Wolfram code (a nonnegative integer $R \in [0, p^{r+l+1}]$) and the neighborhood parameters p , l and r directly. For example, the celebrated Wolfram's rule 110 takes the simple form

$$x_{t+1}^j = \mathbf{d}_2 \left(\sum_{k=-1}^1 2^{k+r} x_t^{j+k}, 110 \right) \quad (16)$$

The maps for all Wolfram's 256 CA with $l = r = 1$ and $p = 2$ are thus simply obtained as

$$x_{t+1}^j = \mathbf{d}_2 \left(\sum_{k=-1}^1 2^{k+r} x_t^{j+k}, R \right) \quad (17)$$

by giving an input $R \in [0, 255]$. As a further illustration, the 'three-color' $p = 3$ CA rule $x_{t+1}^j = \mathbf{d}_3 \left(\sum_{k=-1}^1 3^{k+r} x_t^{j+k}, 741831466113 \right)$ is plotted in Fig. 1 starting from an arbitrary initial condition.

We can now take profit of the results derived in the previous Section for the digit function. Let the number of symbols p have unique prime decomposition into factors p_0, \dots, p_{N-1} as $p = p_0 p_1 \dots p_{N-1}$. Then, by using Eq. (12) in Eq. (15) we obtain

$$x_{t+1}^j = \sum_{h=0}^{N-1} \mathbf{d}_{p_h} \left(\sum_{k=-r}^l p^{k+r} x_t^{j+k}, \frac{R}{(\prod_{m=0}^{h-1} p_m)^{1+\sum_{k=-r}^l p^{k+r} x_t^{j+k}} (\prod_{n=h+1}^{N-1} p_n)^{\sum_{k=-r}^l p^{k+r} x_t^{j+k}}} \right) \prod_{j=0}^{h-1} p_j \quad (18)$$

and thus, by using Eqs. (4) and Eq. (14)

$$\begin{aligned} x_{t+1}^j &= \sum_{h=0}^{N-1} \mathbf{d}_{p_h} \left(0, \frac{R}{p^{\sum_{k=-r}^l p^{k+r} x_t^{j+k}} \prod_{m=0}^{h-1} p_m} \right) \prod_{j=0}^{h-1} p_j \\ &= \sum_{h=0}^{N-1} \mathbf{d}_{p_h} \left(0, \frac{1}{\prod_{m=0}^{h-1} p_m} \sum_{n=0}^{p^{l+r+1}-1} a_n p^{n-\sum_{k=-r}^l p^{k+r} x_t^{j+k}} \right) \prod_{j=0}^{h-1} p_j \end{aligned} \quad (19)$$

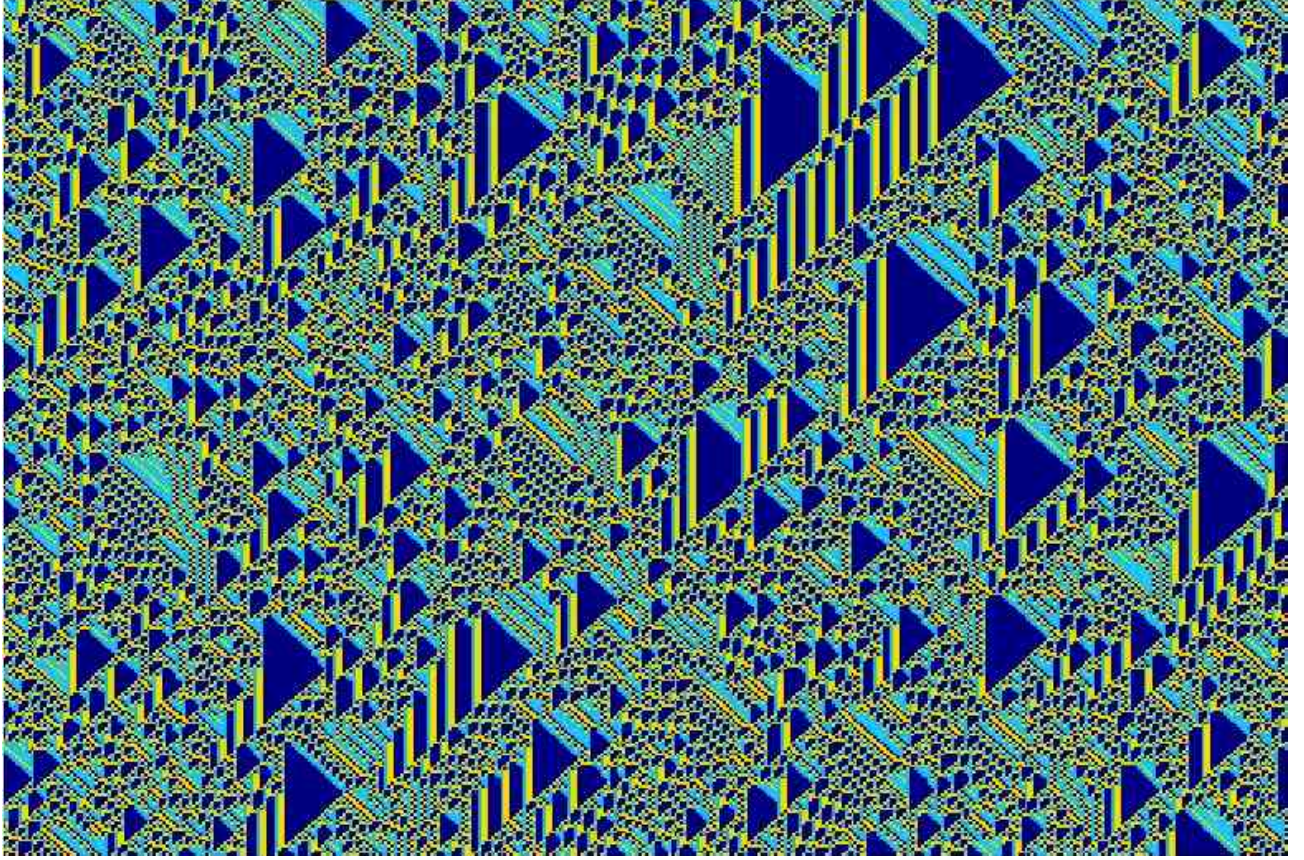


FIG. 1: Spatiotemporal evolution of the rule $x_{t+1}^j = \mathbf{d}_3 \left(\sum_{k=-1}^1 3^{k+r} x_t^{j+k}, 741831466113 \right)$ starting from an arbitrary initial condition on a ring of 400 sites and 300 time steps. Time flows from top to bottom. Periodic boundary conditions are used.

If we compare this result with Eq. (15) (by using also Eq. (4) there)

$$x_{t+1}^j = \mathbf{d}_p \left(0, \frac{R}{p^{\sum_{k=-r}^l p^{k+r} x_t^{j+k}}} \right) = \mathbf{d}_p \left(0, \sum_{n=0}^{p^{l+r+1}-1} a_n p^{n-\sum_{k=-r}^l p^{k+r} x_t^{j+k}} \right) \quad (20)$$

we observe that Eq. (19) can be interpreted at each time as a linear superposition of N CA with Wolfram codes $R/\prod_{m=0}^{h-1} p_m$ each (with $h \in [0, N-1]$) and acting each on p_h symbols. Let us consider $p_0 \geq p_1 \geq \dots \geq p_{N-1}$, each of the different N CA by taking the appropriate digit function of both sides of Eq. (18). Then, we obtain the N different equations

$$\mathbf{d}_{p_0}(0, x_{t+1}^j) = \mathbf{d}_{p_0} \left(0, \frac{R}{p^{\sum_{k=-r}^l p^{k+r} x_t^{j+k}}} \right) \quad (21)$$

$$\mathbf{d}_{\prod_{j=0}^{h-1} p_j}(1, x_{t+1}^j) = \mathbf{d}_{p_h} \left(0, \frac{R}{p^{\sum_{k=-r}^l p^{k+r} x_t^{j+k}} \prod_{m=0}^{h-1} p_m} \right) \quad h = 1, \dots, N-1 \quad (22)$$

Let us, in the following consider, for simplicity $p = p_0 p_1$, with $p_0 \geq p_1$ and let us focus on all CA rules of range $\rho = 2$ (we take, e.g. $l = 0$, $r = 1$ and, hence, the rules ${}^0 R_{p_0 p_1}^1$). Then, Eq. (19) takes in this

case the form

$$x_{t+1}^j = \mathbf{d}_{p_0} \left(0, \frac{R}{(p_0 p_1)^{x_t^{j-1} + p_0 p_1 x_t^j}} \right) + p_0 \mathbf{d}_{p_1} \left(0, \frac{R/p_0}{(p_0 p_1)^{x_t^{j-1} + p_0 p_1 x_t^j}} \right) \quad (23)$$

where Eq. (4) has been used. The CA consists of two independent coupled layers whose evolution that can be written into two separate equations as

$$\mathbf{d}_{p_0}(0, x_{t+1}^j) = \mathbf{d}_{p_0} \left(0, \frac{R}{(p_0 p_1)^{x_t^{j-1} + p_0 p_1 x_t^j}} \right) = \mathbf{d}_{p_0} \left(0, \sum_{n=0}^{(p_0 p_1)^2 - 1} (p_0 p_1)^{n - x_t^{j-1} - p_0 p_1 x_t^j} a_n \right) \quad (24)$$

$$\mathbf{d}_{p_0}(1, x_{t+1}^j) = \mathbf{d}_{p_1} \left(0, \frac{R/p_0}{(p_0 p_1)^{x_t^{j-1} + p_0 p_1 x_t^j}} \right) = \mathbf{d}_{p_1} \left(0, \frac{1}{p_0} \sum_{n=0}^{(p_0 p_1)^2 - 1} (p_0 p_1)^{n - x_t^{j-1} - p_0 p_1 x_t^j} a_n \right) \quad (25)$$

by taking the appropriate digit function on both sides of Eq. (23) and by using Eq. (5) and the fact that $p_1 \leq p_0$. These two equations thus contain the same information as Eq. (23) but allow for separate treatment. Because of the structure of these equations, it may happen that, without decoupling, one of them exhibits a predictable behavior with time while the other does not. Consequently Eq. (23) will display an unpredictable spatiotemporal evolution. The fact that, e.g. $\mathbf{d}_{p_0}(1, x_t^j)$ may display a predictable behavior while $\mathbf{d}_{p_0}(0, x_t^j)$ does not, is a most remarkable one. That this might be the case comes from the fact that, although both these quantities are carried together by the spatiotemporal evolution of x_t^j , they can be made to behave analogously to the different dimensions of a vector. This is best shown with an example, that we provide next.

Let us consider a rule ${}^0R_{12}^1$, i.e. with $p = 12$, $l = 0$, $r = 1$ and range $\rho = l + r + 1 = 2$ with Wolfram code

$$R = \sum_{n=0}^{143} a_n 12^n \quad (26)$$

and with rule vector

$$\begin{aligned} \mathbf{a} \equiv (a_0, a_1, \dots, a_{143}) = & (0, 1, 2, 3, 4, 5, 6, 7, 8, 9, 10, 11, 1, 0, 4, 5, 2, 3, 7, 6, \\ & 10, 11, 8, 9, 2, 5, 0, 4, 3, 1, 8, 11, 6, 10, 9, 7, 3, 4, 5, 0, 1, 2, 9, 10, 11, 6, 7, 8, \\ & 4, 3, 1, 2, 5, 0, 10, 9, 7, 8, 11, 6, 5, 2, 3, 1, 0, 4, 11, 8, 9, 7, 6, 10, 6, 7, 8, 9, 11, \\ & 10, 0, 1, 2, 3, 5, 4, 7, 6, 10, 11, 9, 8, 1, 0, 5, 4, 2, 3, 8, 11, 6, 10, 7, 9, 2, 4, 0, 5, \\ & 3, 1, 9, 10, 11, 6, 8, 7, 3, 5, 4, 0, 1, 2, 10, 9, 7, 8, 6, 11, 4, 2, 3, 1, 0, 5, 11, 8, 9, \\ & 7, 10, 6, 5, 3, 1, 2, 4, 0) \end{aligned} \quad (27)$$

This rule provides the map $x_{t+1}^j = {}^0R_{12}^1(x_t^j, x_t^{j-1}) \equiv x_t^j * x_t^{j-1}$ which is described by Eq. (23) and which shows that the CA rule ${}^0R_{12}^1$ above can be understood as a binary operator (law of composition) $*$ which is both non-commutative and non-associative but which is alternating, satisfying the Moufang identities [18] for any $x, y, z \in [0, 11]$ integers

$$z * (x * (z * y)) = ((z * x) * z) * y \quad (28)$$

$$x * (z * (y * z)) = ((x * z) * y) * z \quad (29)$$

$$(z * x) * (y * z) = (z * (x * y)) * z \quad (30)$$

$$(z * x) * (y * z) = z * ((x * y) * z) \quad (31)$$

However, if $x = z$, $x = y$ or $y = z$, the resulting subalgebra is associative. The action of this rule on x_t^j and x_t^{j-1} to output x_{t+1}^j is better understood if we tabulate all such output values $x_t^j * x_t^{j-1}$ for x_t^j in the rows and x_t^{j-1} in the columns of the table:

*	0	1	2	3	4	5	6	7	8	9	10	11
0	0	1	2	3	4	5	6	7	8	9	10	11
1	1	0	4	5	2	3	7	6	10	11	8	9
2	2	5	0	4	3	1	8	11	6	10	9	7
3	3	4	5	0	1	2	9	10	11	6	7	8
4	4	3	1	2	5	0	10	9	7	8	11	6
5	5	2	3	1	0	4	11	8	9	7	6	10
6	6	7	8	9	11	10	0	1	2	3	5	4
7	7	6	10	11	9	8	1	0	5	4	2	3
8	8	11	6	10	7	9	2	4	0	5	3	1
9	9	10	11	6	8	7	3	5	4	0	1	2
10	10	9	7	8	6	11	4	2	3	1	0	5
11	11	8	9	7	10	6	5	3	1	2	4	0

This table corresponds to the Cayley table of the smallest Moufang loop $M_{12}(S_3, 2)$ [19] of order 12 (see [20] for a classification of small Moufang loops). The Moufang identities above are satisfied, as can be readily checked. Because of the breaking of the associative property, we expect that the behavior will be chaotic/unpredictable for an arbitrary initial condition, very much as Wolfram's rule 30 (reproduced by Eq. (17 with $R = 30$) is chaotic [1]. However, because of the presence of associative subalgebras, we also expect a certain degree of order and predictability, which we are about to disentangle.

We now note that we have $p = 12 = 6 \cdot 2$ so that we can consider the decomposition presented above, Eq. (23) with $p_0 = 6$ and $p_1 = 2$, and study separately Eqs. (24) and (25) in order to get insight in the dynamics. It then becomes apparent from this table that Eq. (25) takes the simple form

$$\mathbf{d}_6(1, x_{t+1}^j) = \mathbf{d}_2(0, \mathbf{d}_6(1, x_t^j) + \mathbf{d}_6(1, x_t^{j-1})) \equiv \mathbf{d}_6(1, x_t^j) +_2 \mathbf{d}_6(1, x_t^{j-1}) \quad (32)$$

where $+_2$ denotes addition modulo 2 [13, 16]. Why this is so can be easily understood from the table Cayley table above. For if we apply the operation $\mathbf{d}_6(1, y)$ to every entry in the table, we obtain the reduced simple table

$+_2$	0	1
0	0	1
1	1	0

where the outputs $\mathbf{d}_6(1, x_{t+1}^j)$ are given for the row values $\mathbf{d}_6(1, x_t^j)$ and the column values $\mathbf{d}_6(1, x_t^{j-1})$. This corresponds to addition modulo 2 operation. Thus, technically speaking, the operation $\mathbf{d}_6(1, y)$ provides an homomorphism of the Moufang loop $M_{12}(S_3, 2)$ to the additive group \mathbb{Z}_2 of the integers modulo 2.

The meaning of the layer described by Eq. (25), which reduces in this case to Eq. (32) is now clear to explain. If one considers the sets of values $S_0 \equiv \{0, 1, 2, 3, 4, 5\}$ and $S_1 \equiv \{6, 7, 8, 9, 10, 11\}$ then Eq. (32) specifies at each time to which set belongs x_{t+1}^j from the information of those of x_t^j and x_t^{j-1} . Note that, if $\mathbf{d}_6(1, x_{t+1}^j) = 0$ then $x_t^j \in S_0$ and if $\mathbf{d}_6(1, x_{t+1}^j) = 1$ then $x_t^j \in S_1$. Equation (32) establishes that, at time $t+1$ the value x_{t+1}^j belongs to set S_1 if either x_t^j or x_t^{j-1} belong to S_1 , but not both. A most remarkable fact is that *we can exactly predict at every time to which set belongs x_t^j , if we know the initial condition x_0^j* . This is given by [13, 21, 22]

$$\mathbf{d}_6(1, x_t^j) = \mathbf{d}_2 \left(0, \sum_{k=0}^t \binom{t}{k} \mathbf{d}_6(1, x_0^{j+k-t}) \right) \quad (33)$$

as can be easily shown by induction. If in the initial condition there is only one location for which $\mathbf{d}_6(1, x_0^j) = 1$, $j = 0$ say, this equation reduces to a Pascal triangle modulo 2, which, in fact, is equal to a Sierpinsky triangle [13, 21, 22]

$$\mathbf{d}_6(1, x_t^j) = \mathbf{d}_2 \left(0, \binom{t}{k} \right) \equiv \binom{t}{k} \pmod{2} \quad (34)$$

The behavior of Eq. (24) is far more complex and no shortcut for the trajectory seems possible. Thus, the full evolution dictated by Eq. (23) is unpredictable as well. The conclusion of all this is that *while we cannot predict the actual value of x_t^j in this case, we can exactly predict at every time, from Eq. (33), to which set S_0 or S_1 belongs the value of x_t^j* .

We have performed numerical calculations of the spatiotemporal evolution of the CA above, given by Eq. (26) and Eq. (27). Because the Wolfram code being an enormous number, it is better to work in practice with the rule vector given by Eq. (27) and with the universal map for CA derived in [15]

$$x_{t+1}^i = {}^l R_p^r(x_t^i) = \sum_{n=0}^{p^{r+l+1}-1} a_n \mathcal{B} \left(n - \sum_{k=-r}^l p^{k+r} x_t^{i+k}, \frac{1}{2} \right) \quad (35)$$

where

$$\mathcal{B}(x, y) \equiv \frac{1}{2} \left(\frac{x+y}{|x+y|} - \frac{x-y}{|x-y|} \right) = \frac{1}{2} (\text{sign}(x+y) - \text{sign}(x-y)) \quad (36)$$

is the \mathcal{B} -function for any real numbers x, y . Eq. (35) is equivalent to Eq. (15) and overcomes the problem of large powers of p (in the denominators within the digit function). In Eq. (35) we thus take $p = 12$, $l = 0$, $r = 1$ and the a_n given by Eq. (27). In Fig. 2 we show the spatiotemporal evolution of x_t^j (left column), $\mathbf{d}_6(0, x_t^j)$ (middle column), $\mathbf{d}_6(1, x_t^j)$ (right column) calculated from Eqs. (23) (i.e. Eq. (35) with the above parameters), (24) and (25) respectively and for initial conditions corresponding to $x_0^j = 0$ for $j > 11$ and $x_0^j = 12 - j$ for $0 \leq j \leq 11$ (top panels) and for a random initial condition (bottom panels). We observe that, although for x_t^j (left column) and $\mathbf{d}_6(0, x_t^j)$ (middle column) the spatiotemporal evolution is unpredictable, the one of the $\mathbf{d}_6(1, x_t^j)$ (right column) is exactly predictable and given by Eq. (33) in both cases: The light regions correspond to $\mathbf{d}_6(1, x_t^j) = 1$ and the dark regions to $\mathbf{d}_6(1, x_t^j) = 0$. Furthermore, we see that there certainly exist subtle correlations between the chaotic signal $\mathbf{d}_6(0, x_t^j)$ and the predictable one $\mathbf{d}_6(1, x_t^j)$, although these do not affect the predictable character of $\mathbf{d}_6(1, x_t^j)$. The two signals are not independent, they are correlated in a complex way through the spatiotemporal dynamics Eq. (15), as reflected also in the evolution of $\mathbf{d}_6(0, x_t^j)$ in the top middle panel of Fig. 2. Still, with the method presented in this paper, both layers can be disentangled and

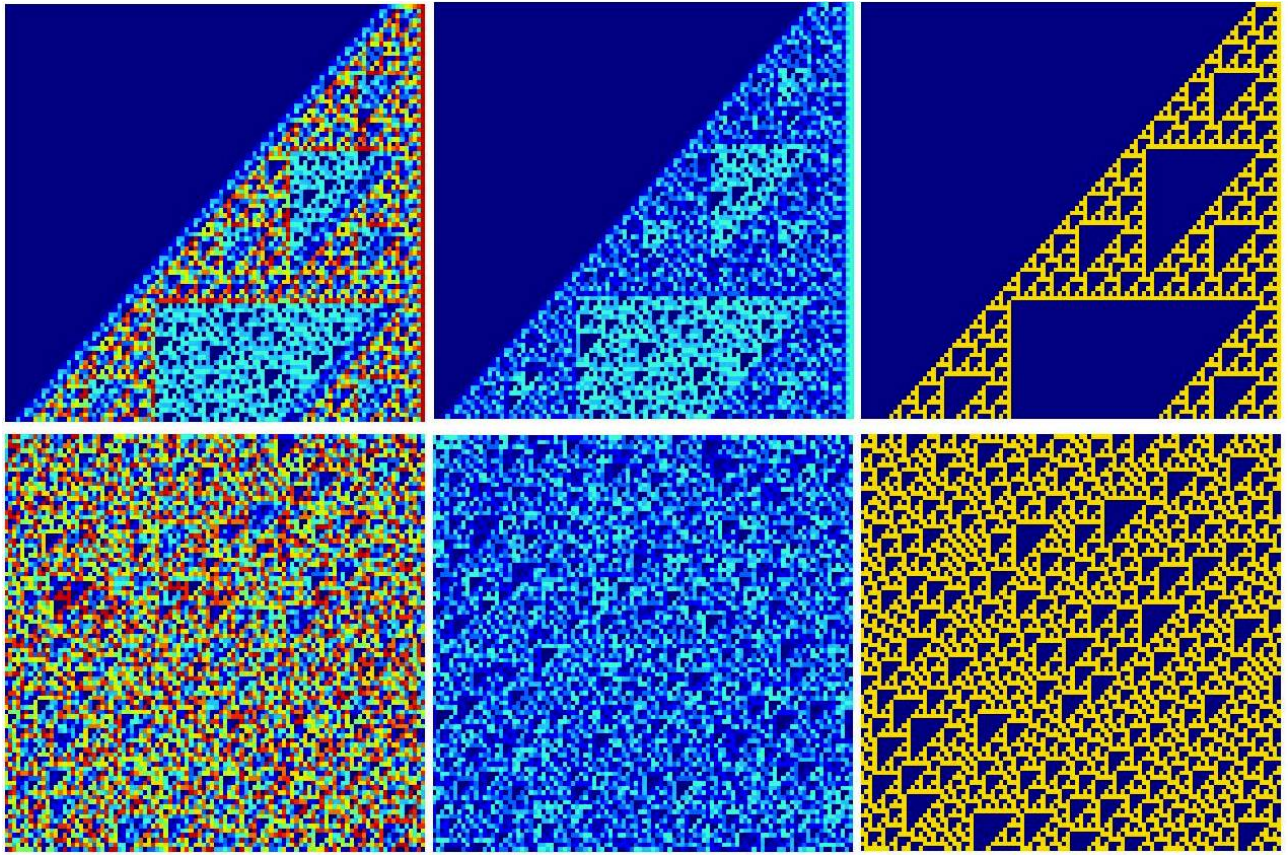


FIG. 2: Spatiotemporal evolution of x_t^j (left column), $\mathbf{d}_6(0, x_t^j)$ (middle column), $\mathbf{d}_6(1, x_t^j)$ (right column) calculated from Eqs. (23) (see text), (24) and (25) respectively, for the CA rule given by Eq. (27) and for initial conditions corresponding to $x_0^j = 0$ for $j > 11$ and $x_0^j = 12 - j$ for $0 \leq j \leq 11$ (top panels) and for a random initial condition (bottom panels). We observe that, although for x_t^j (left column) and $\mathbf{d}_6(0, x_t^j)$ (middle column) the spatiotemporal evolution is unpredictable, the one of the $\mathbf{d}_6(1, x_t^j)$ (right column) is exactly predictable and given by Eq. (33) in both cases: The light regions correspond to $\mathbf{d}_6(1, x_t^j) = 1$ and the dark regions to $\mathbf{d}_6(1, x_t^j) = 0$. Time flows from top to bottom in each panel. Periodic boundary conditions are used, $j \in [1, 100]$ and time $t \in [0, 88]$.

treated separately. If we are only interested in knowing the set S_0 or S_1 taken by x_t^j we certainly can answer this exactly, even when we cannot know which specific element of these sets x_t^j equals to. Note that this has nothing to do with coarse graining as discussed in [11, 12]: Even when we can simplify the complex dynamics to a more simple CA, we are always addressing here the fine details of the trajectory and *not* a coarse grained version of it.

IV. CONCLUSIONS

In this article we have presented a method to decompose any nonlinear CA acting on an alphabet of p symbols into a superposition of N CAs, acting each on a number of symbols p_h , $h = 0, \dots, N-1$ that is one of the factors in the prime factor decomposition of p . Since this prime factor decomposition

is unique (by the celebrated Euclid theorem) so is also this CA decomposition unique for each CA in rule space. This general result applies to *all* CA in rule space and has lead us to discover a new class of dynamical systems that we have termed *semipredictable dynamical systems*: Although their overall spatiotemporal dynamics is unpredictable certain traits of the evolution can be exactly predicted. We have given an explicit example of semipredictable system, a rule of range $\rho = 2$ acting on $p = 12$ symbols and for which the rule table has the structure of the smallest Moufang loop. We have seen that, in spite of the spatiotemporal dynamics being chaotic and unpredictable, the CA can be decomposed into two layers, one of them strongly chaotic and the other displaying an entirely predictable spatiotemporal evolution for any initial condition. This is a remarkable fact since it shows that a chaotic signal can carry with itself coherent information that can be extracted from a digital analysis of the signal.

The semipredictable dynamical systems presented here may find applications in the modeling of biological and complex systems. Most complex systems found in nature possess both predictable and unpredictable traits. For example, a certain disease on a complex organism can have a predictable evolution, with the dynamics of the complex organism that acts as host being unpredictable in many details that are relevant to the overall dynamics. By means of our model we have seen that, even when predictable and unpredictable layers describing the dynamics are correlated, and hence not totally independent, they have sometimes robust features (closed substructures) that warrant their separate tractability and solvability.

- [1] S. Wolfram, *A New Kind of Science* (Wolfram Media Inc., Champaign, IL, 2002).
- [2] G. A. Hedlund, Math. Systems Theory **3**, 320 (1969).
- [3] A. Adamatzky, *Identification of Cellular Automata* (Taylor and Francis, London, 1994).
- [4] A. Wuensche and M. Lesser, *The Global Dynamics of Cellular Automata* (Addison-Wesley, Reading, MA, 1992).
- [5] L. O. Chua, *A Nonlinear Dynamics Perspective of Wolfram's New Kind of Science, vol. I-VI* (World Scientific, Singapore, 2013).
- [6] J. Kari, Theor. Comput. Sci. **334**, 3 (2005).
- [7] B. Chopard and M. Droz, *Cellular Automata Modeling of Physical Systems* (Cambridge University Press, Cambridge, UK, 2005).
- [8] L. B. Kier, P. G. Seybold, and C.-K. Cheng, *Modeling Chemical Systems using Cellular Automata* (Springer, New York, 2005).
- [9] T. Toffoli, Physica D **10**, 117 (1984).
- [10] H. Meinhardt, *The Algorithmic Beauty of Sea Shells* (Springer, Heidelberg, 2003).
- [11] N. Israeli and N. Goldenfeld, Phys. Rev. Lett. **92**, 074105 (2004).
- [12] N. Israeli and N. Goldenfeld, Phys. Rev. E **73**, 026203 (2006).
- [13] V. García-Morales, Phys. Rev. E **88**, 042814 (2013), nlin/1310.1380.
- [14] L. C. d. S. M. Ozelim, A. L. B. Cavalcante, and L. P. d. F. Borges, Complex Systems **21**, 283 (2013).
- [15] V. García-Morales, Phys. Lett. A **376**, 2645 (2012).
- [16] V. García-Morales, Phys. Lett. A **377**, 276 (2013).

- [17] V. García-Morales, Found. Phys. **45**, 295 (2015), physics.gen-ph/1401.0963.
- [18] R. Moufang, Math. Ann. **110**, 416 (1935).
- [19] O. Chein and H. O. Pflugfelder, Arch. Math. **22**, 573 (1971).
- [20] O. Chein, Trans. Amer. Math. Soc. **188**, 31 (1974).
- [21] H. O. Peitgen, H. Jürgens, and D. Saupe, *Chaos and Fractals* (Springer Verlag, New York, 2004).
- [22] S. Wolfram, Amer. Math. Mon. **91**, 566 (1984).